Urbanization vs climate drivers: investigating changes in fluvial floods in Poland

Nelson Venegas-Cordero[1], Luis Mediero[2], Mikołaj Piniewski[1]

[1] Department of Hydrology, Meteorology and Water Management, Warsaw University of Life Sciences, Nowoursynowska 166, 02-787, Warsaw, Poland.

[2] Department of Civil Engineering: Hydraulics, Energy and Environment, Universidad Politécnica de Madrid, 28040 Madrid, Spain.

Corresponding author: Mikołaj Piniewski, mikolaj_piniewski@sggw.edu.pl

Abstract

Fluvial floods are one of the most severe natural hazards. Changes in flood behaviour result from an interplay of climatic and human factors. Urbanization, with increasing land imperviousness, is the most critical human factor. This study investigates the effect of urbanization vs climate drivers on river floods in Poland, using the paired catchment approach. We used daily river flow data from 1975 to 2020 for four selected urban catchments and their non-urban counterparts as well as extreme precipitation, soil moisture, and snowmelt data generated from the process-based SWAT model. Changes in impervious areas were assessed using two state-of-the-art Copernicus products, revealing a consistent upward trend in imperviousness across all selected urban catchments. We employed a range of statistical methods: the Pettitt test, the Mann Kendall (MK) multitemporal test, the Poisson regression test, multi-temporal correlation analysis and multiple linear regression to assess changes in the magnitude and frequency of floods and flood drivers. The MK test results showed a contrasting behaviour between urban (increases) and non-urban (no change) catchments for three of four analysed catchment pairs. Flood frequency increased significantly in only one urban catchment. Multiple regression analysis revealed complex that non-urban catchments consistently exhibited stronger relationships between floods and climate drivers than the urban ones, although the results of residual analysis were not statistically significant. In summary,

the evidence for the impact of urbanization on floods was found to be moderate. The results emphasize the importance of considering both hydrometeorological and human-induced factors when assessing river flood dynamics in Poland.

Keywords

Flood; Extreme precipitation; Soil moisture excess; Snowmelt; Peak-over-threshold; Imperviousness.

1. Introduction

River floods are usually generated by intense and long-duration precipitation (or short-duration in small river basins). Floods have caused substantial property damage and casualties worldwide, which could increase as climate change projections have indicated increases in the frequency and intensity of extreme precipitation events over large parts of the world (Kundzewicz et al., 2014; Madsen et al., 2014; Prein et al., 2017; Tabari, 2020). In addition, studies have mentioned that around 75% of the population of the European Union is settled in urban areas, with an expected increase of urban extension for the future. This expansion has intensified the economic and human consequences, as well as exposure to hazards such as river floods (Bulti and Abebe, 2020; Depietri et al., 2012; Guerreiro et al., 2018; Hebbert, 2012; Mediero et al., 2022; Skougaard Kaspersen et al., 2017).

Human activities, particularly urbanization and changes in land use, significantly modify catchment characteristics by increasing impermeable surfaces (soil sealing). This reduces precipitation absorption during storms, leading to increased fast runoff processes (Bian et al., 2020; Du et al., 2015; Smith et al., 2023). These alterations, in conjunction with factors such as precipitation, soil moisture excess, snowmelt, and others, can lead to fluctuations in flows and therefore the magnitude of floods can be higher or lower (Davenport et al., 2020; Hodgkins et al., 2017; Tramblay et al., 2019; Venegas-Cordero et al., 2022; Venegas-Cordero et al., 2023). In recent years, urban areas worldwide have faced flooding events triggered

by heavy precipitation (Francipane et al., 2021; Hoeppe, 2016; Mou et al., 2022; Wang et al., 2019; Wasko and Nathan, 2019). This issue is further compounded by global warming, which is expected to intensify the hydrological cycle, resulting in more frequent and intense precipitation events on a global scale (Allan et al., 2020; Brunner et al., 2021; Giorgi et al., 2019; Tabari, 2020).

Various studies have recently examined the impact of land used change or urbanization on floods (Bayazıt et al., 2021; Beckers et al., 2013; Brody et al., 2014; Skougaard Kaspersen et al., 2017). A range of different methods may be used to this end, for example paired-catchment studies (Requena et al., 2017; Prosdocimi et al., 2015; Salavati et al., 2016; Shao et al., 2020) or hydrological modelling (Jodar-Abellan et al., 2019; Gao et al., 2020; Zhang et al, 2020). In a study that attributed the urbanization effect on flood events using the paired-catchment approach in the UK, Prosdocimi et al. (2015) found a great influence of increased urbanization levels on high flow occurrences, particularly during the summer season. As urban areas expand, heavy or prolonged precipitation events can cause faster water flow due to various reasons (Fletcher et al., 2013; Kishtawal et al., 2010; McGrane, 2016; Skougaard et al., 2017). In addition, a study in Mediterranean basins (SE Spain) used the SWAT model to show that flash flood risks have raised due to changes in land use, particularly affected by urban expansion (Jodar-Abellan et al., 2019).

A variety of studies have dealt with the topic of urbanization effect on floods in Poland, taking different perspectives (Pińskwar et al., 2023; Szeląg et al., 2021; Szwagrzyk et al., 2018). For example, Pińskwar et al. (2023), studied the interventions of the State Fire Service units at the west of Warsaw (Wielkopolska region) in urban floods and concluded that this area is most at risk in case of extreme precipitation and therefore at high risk of flash floods. Then, a probabilistic methodology was also applied to study the interactions between changes in rainfall dynamics and impervious areas in different urban watersheds in Poland. It was shown that the dynamics of land use changes (urbanization) have a strong impact on the number of floods (Szeląg et al., 2021). Conclusively, Szwagrzyk et al. (2018) showed the impact of projected land use changes on flood risk in the southern polish mountain range and concluded that urban areas are

expected to increase in existing flood-prone zones. Therefore, a substantial increase in estimated economic losses due to potential flooding can be expected.

Finally, in this study, the main objective is to assess the effect of urbanization on fluvial floods in Poland. To this end, we integrate high-resolution, spatio-temporal data on soil imperviousness with observed river flow data as well as modelled data on climatic flood drivers over the period 1951-2020. As for the methods, we combine the paired-catchment approach, the annual maximum flow (AMF) and peak-over-threshold (POT) approaches, the multi-temporal trend analysis and multiple linear regression. The analysis is carried out for eight small and medium-sized catchments around Poland with variable degrees of urbanization.

2. Data and methods

2.1 Imperviousness data

In this research, we collected imperviousness data for the entire territory of Poland from two Copernicus products: (1) the Global Human Settlement (GHS) layer, specifically capturing the GHS built-up data for the period 1975-2020 and (2) the 'High Resolution Layer (HRL): Imperviousness Degree' dataset covering the period 2006-2018. The first dataset is a freely available open surface grid with global coverage, derived from a fusion of Sentinel-2 composites and Landsat imagery in five-year intervals (Pesaresi and Politis, 2022). The GHS-BUILT-S product used in this study depicts the distribution of the built-up surfaces (ranging from 0 to 10 000 m^2) estimates for each grid cell at 100 m resolution.

The second one, developed by the European Environment Agency (EEA), is designed to detect the spatial distribution and temporal evolution of artificially sealed areas at a continental scale. The product is derived from high-resolution satellite imagery (ESA's Sentinel-1 and Sentinel-2 satellites). The HRL Imperviousness Density product used in this study provides data on sealing density ranging from 0% to 100% at 20 m resolution for the period 2006-2018 with a three-year interval.

To facilitate comparison between both products, the GHS-BUILT-S raster was divided by 100 which resulted in the same unit as the HRL layer (% of imperviousness). We applied the zonal statistics functions in ArcGIS (average value across all pixels inside the catchment) to calculate catchment-averaged imperviousness indicators.

2.2 Hydrometeorological data

Daily discharge data was extracted from the Polish Institute of Meteorology and Water Management-National Research Institute (IMGW-PIB). Building on the study of Venegas-Cordero et al. (2023), we considered three hydroclimate variables, (precipitation, snowmelt and soil moisture) as potential flood generation mechanisms over Poland. Relevant data were derived from the simulated water balance dataset (PL-SWAT-51_20) developed by Marcinkowski et al. (2021) for the area of Poland. These simulations were generated using a semi-distributed, process-based hydrological model SWAT, driven by the G2DC-PL+ gridded climate dataset (Piniewski et al., 2021). For more information about the PL+ SWAT dataset, readers can refer to Marcinkowski et al. (2021).

2.3 Paired catchment selection

In the first step, we investigated the evolution of impervious surface in Poland based on GHS and HRL products for their respective periods (Fig. 1; Table 1). The results highlight a significant shift in imperviousness patterns in Poland according to both data sources. The gradual transition from non-impervious to impervious areas is clearly shown, with a consistent increase in impervious surfaces. However, both the actual value of average imperviousness and the rate of its increase are significantly higher for the HRL product , with values of 16.71% and 21.24% for 2006 and 2018, respectively.

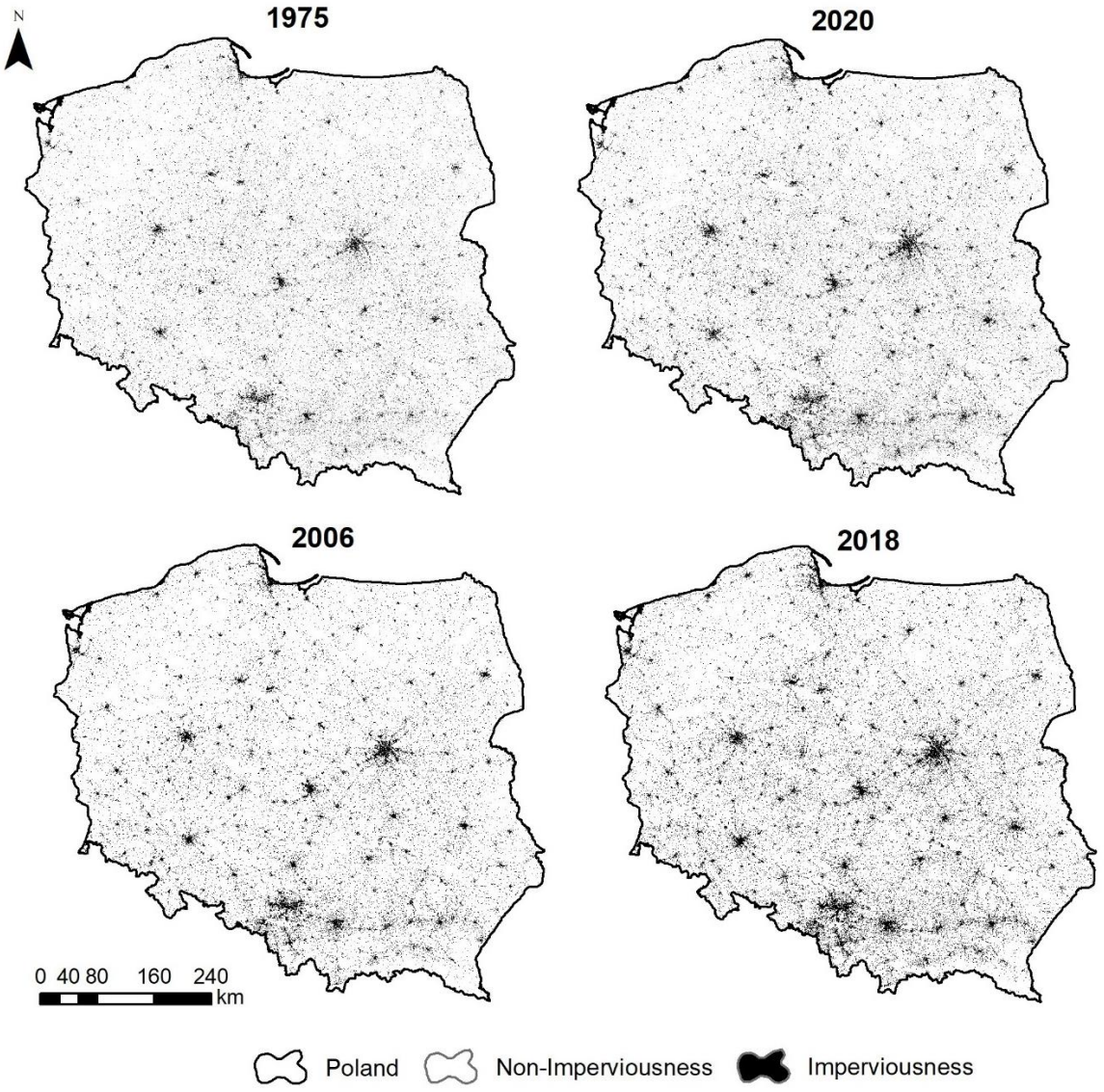

113

114 Fig. 1: Evolution of the Imperviousness in Poland according to the GHS (1975-2020) and HRL (2006-2018)

115 products.

116 Table 1: Imperviousness and non-imperviousness area percentages in Poland (1975-2020 and 2006-2018).

Year	Non-impervious (%)	Impervious (%)
	GHS	
1975	87.79	12.21
2020	83.48	16.52
	HRL	
2006	83.29	16.71
2018	78.76	21.24

Following the country-scale analysis of imperviousness, our workflow focused on selection of pairs of neighbouring catchments with contrasting imperviousness characteristics. We thus adopted the widely used paired-catchment approach, a classical technique employed in hydrology, which entails comparing the response of two catchments with similar physical characteristics (Bosch and Hewlett, 1982; Kreibich et al., 2017; Prosdocimi et al., 2015; Van Loon et al., 2019). In this approach, one of the catchments is considered as a treatment (in our case with high imperviousness, further denoted as "urban") and the other remains as a control (in our case with low imperviousness, further denoted as "non-urban"). Comparison of flood response between neighbouring catchments allows us to attribute the differences to urbanization as the main factor differing both catchments, although confounding factors such as precipitation certainly exist.

In this context, catchment selection procedure aimed at maximizing the contrasting imperviousness characteristics of pairs of neighbouring catchments, while maximizing the availability of flow record. In this process we have used both HRL and GHS raster in conjunction with vector layers of catchments located upstream of the candidate flow gauging stations, taking into account flow data availability. We assumed that capturing the effect of imperviousness on floods will be more likely in small catchments, as changes in large catchments could be driven by multiple variables, such as the spatial variability of precipitation. Hence, the upper limit for catchment area was set to 1 000 km^2. The minimum flow record length was set to 30 years. An intersection of imperviousness and catchment layers allowed to shortlist catchments having both high imperviousness and high rate of its change. In the next step, we identified catchments with low imperviousness (and sufficient flow record length) in the 50 km proximity of each urban catchment. We prioritized catchments with similar areas as the urban ones.

Table 2: Basic catchment characteristics and flow data availability.

Pair ID	Gauge name	River name	Type	Code	Area (km^2)	Elevation (m)	Starting year	Ending year	Missing data
1	Krępa	Glaźna	Urban	U1	73.7	61.7	1980	2020	-
	Pogorzelice	Pogorzelica	Non-Urban	N1	91.2	107.8	1980	2020	-
2	Kuźnica Skakawska	Niesób	Urban	U2	244.7	168.6	1971	2020	-
	Gorzów Śląski	Prosna	Non-Urban	N2	164.5	207.8	1971	2020	-
3	Lesiów	Mleczna	Urban	U3	338.9	164.2	1973	2020	2002
	Bzin	Kamienna	Non-Urban	N3	276.2	269.9	1973	2020	-
4	Szabelnia	Brynica	Urban	U4	496.6	283.7	1951	2020	-
	Krupski Młyn	Mała Panew	Non-Urban	N4	665.8	268.8	1951	2020	-

The above procedure resulted in the final selection of four pairs of catchments (Table 2). They are ordered by their increasing imperviousness index, from U1 (1.4% in 2020) to U4 (7.3% in 2020). The first pair was located in northern Poland, while the other three were clustered in southern part of the country (Fig. 2; see Fig. S1 in Electronic Supplementary Material for a similar figure based on HRL data). For each pair, the difference in imperviousness indicators (both the actual state and the rate of change) between the urban and non-urban catchments is evident. It should also be noted that the term non-urban should not be taken literally, as these catchments obviously have a certain area of impervious surfaces. As shown in Figure 2, for each pair the respective indices are considerably higher for urban catchments, compared with non-urban ones. Selected catchments also exhibit variations in size (ranging from 74 to 497 km^2) and mean elevation (ranging from 62 to 284 m asl). Flow record length ranges from 70 years (pair 4) to 41 years (pair 1), and for each case it reaches year 2020. Thus, there is a good overlap between the flow record time windows and the period of GHS product temporal coverage.

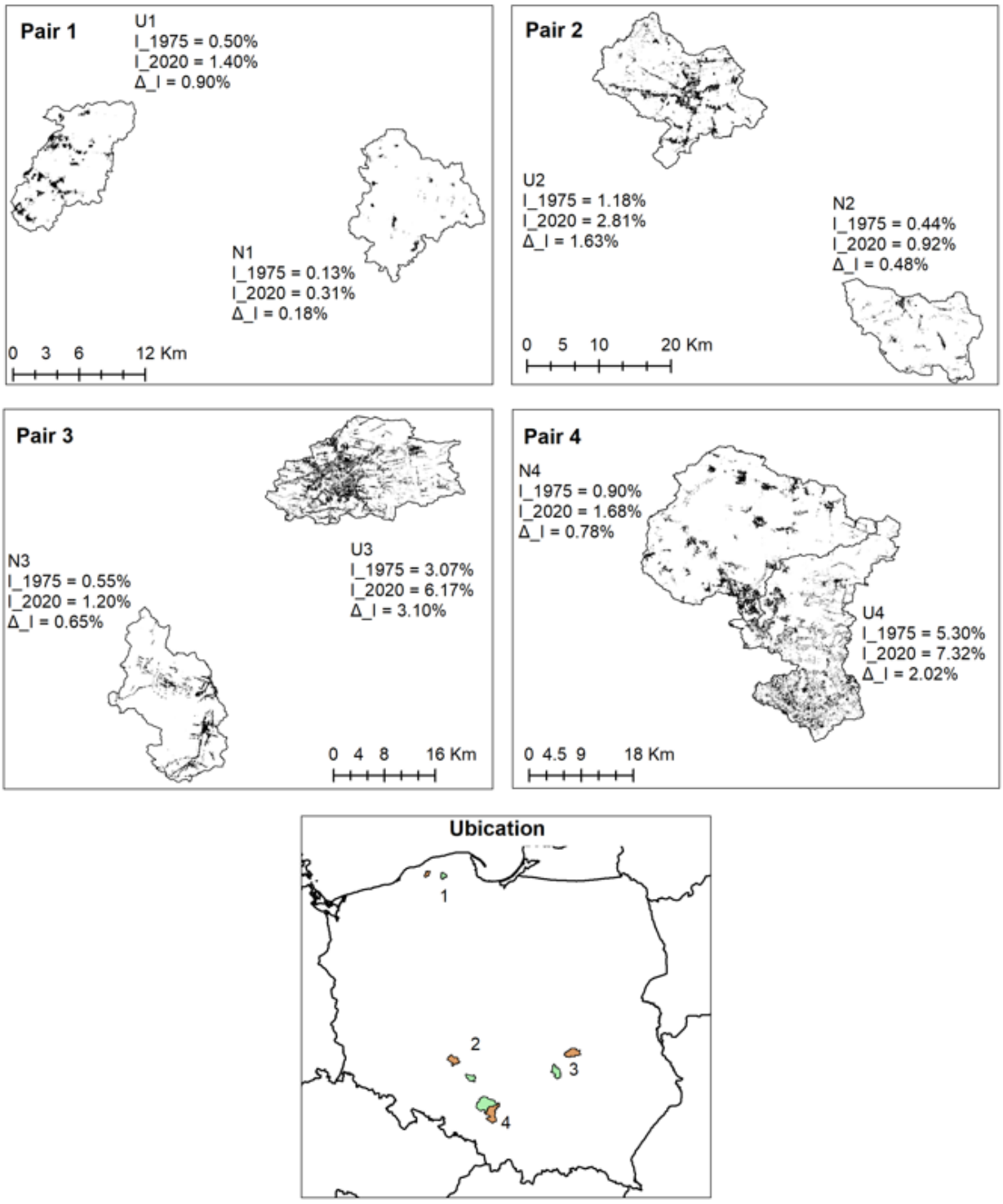

Fig. 2: Location of four pairs of catchments used in this study; Urban and non-urban catchments are shown in orange and green, respectively. Evolution of the imperviousness rate between 1975 (I_1975) and 2020 (I_2020) and relative change (Δ _I) is shown for each pair.

2.4 Flood and climate indices

This study uses two different approaches for extracting flood time series: annual maximum river discharge (Q_{MAX}) and peaks-over-threshold (POT). The main goal is to detect if increasing imperviousness in urban catchments translates into increasing magnitude or frequency of floods. However, we also include other potential drivers of flood change, such as extreme precipitation, snowmelt and soil moisture excess (Berghuijs et al., 2019; Venegas-Cordero et al., 2023). The flood and climate indices considered in the study are listed in Table 3.

Table 3: Flood and climate indices.

Index	Abbreviation	Description
Annual maximum river discharge (m^3/s)	Q_{MAX}	Maximum daily discharge in each year
Peak-over-threshold magnitude (m^3/s)	POT3	Hydrograph peaks that exceed a given threshold with an average of three exceedances per year
Peak-over-threshold frequency (m^3/s)	POT3F	Annual number of peaks that exceed the given threshold per year
Annual maximum 3-day precipitation (mm)	PCP_{MAX}	Maximum 3-day precipitation in each year
Annual maximum soil moisture excess (mm)	SME_{MAX}	Maximum daily soil moisture excess in each year
Annual maximum snowmelt (mm)	SMN_{MAX}	Maximum daily snowmelt in each year

PCP_{MAX} represents the 3 day-maximum amount recorded in a year. While, SME_{MAX} is based on the maximum value recorded in a year, where it was calculated based in Venegas-Cordero et al. (2023) with the following equation:

$$SME = PCP - SM_{MAX} - SM$$

where SME is the soil moisture excess, PCP is the daily precipitation, SM_{MAX} is the soil moisture storage capacity (fixed to 125 mm) as Berghuijs et al. (2019) and Venegas et al. (2023), and SM is the daily soil moisture amount. Furthermore, SMN_{MAX} denotes the highest accumulation observed in a given year.

Q_{MAX} represents the maximum discharge recorded in a given year. In contrast, POT is based on the extraction of hydrograph peaks exceeding a predefined threshold. The POT approach extracts the largest peaks in the series regardless when they occurred, not including smaller flood events considered in annual maximum series that are the largest in a given hydrological year but smaller than the threshold (Lang et al., 1999; Madsen et al., 1997; Mangini et al., 2018; Venegas-Cordero et al., 2022). We assess flood magnitude changes using both Q_{MAX} and POT, with a specific emphasis on the POT approach for flood frequency analysis.

The POT method is employed to effectively detect variations in flood frequency, owing to its ability to identify multiple flood events within a given year. To achieve this, we used a predefined threshold, which allowed us to detect an average of three events per year. Several flood analysis worldwide have employed thresholds based on percentiles (Jiang et al., 2022; Mallakpour and Villarini, 2015; Venegas-Cordero et al., 2022; Villarini et al., 2011). Furthermore, to prevent the double counting of two or more peaks that belong to the same flood event, we selected the largest peak within a 15-day period (Jiang et al., 2022; Mallakpour and Villarini, 2015).

2.5 Statistical analysis

The Pettitt test is a non-parametric method designed to detect change points in the mean or median in a time series. This approach is applied to the Q_{MAX} and POT3 time series extracted previously. The p-values were calculated for the test statistic using Pettitt's approximated limiting distribution, which is specifically designed for continuous variables (Pettitt, 1979; Villarini et al., 2009). A significance level of 5% is considered.

Trends in flood magnitude indicator time series of Q_{MAX} and POT3 were detected using the Mann-Kendall (MK) test (Kendall, 1975; Mann, 1945). The Sen's slope test is used to assess trend magnitudes (Sen, 1968). The MK test is designed to identify the presence of monotonic either upward or downward trends. The

198 Sen's slope is based on the median slope between all ordered pairs of observations for a given time series
199 (Piniewski et al., 2018; Venegas-Cordero et al., 2023). Moreover, the MK test is a suitable method for the
200 non-normal distribution characteristics of hydrological datasets (Kundzewicz and Robson, 2004; Mediero
201 et al., 2014; Venegas-Cordero et al., 2022).

202 The Poisson regression test was applied to POT3F time series as reported in previous publications (Aryal
203 et al., 2018; Mangini et al., 2018; Venegas-Cordero et al., 2022; Vormoor et al., 2016). We analyse
204 sensitivity of the period considered in the time series in both the MK test detected trends for flood
205 magnitude and the Poisson regression for flood frequency by using the multi-temporal trend analysis,
206 which detects trends for all possible combinations of starting and ending years in the time series
207 (Hannaford et al., 2013; Hannaford et al., 2021; Mediero et al., 2014; Ruiz-Villanueva et al., 2016). The
208 minimum time window was set to 20 years.

209 In this study, the MK test is based on the following equations as shown in Venegas-Cordero et al.
210 (2023):

211 $$S = \sum_{i=1}^{n-1} \sum_{j=1+1}^{n} sgn(X_j - X_i) \quad (2)$$

212 $$sgn(X_j - X_i) = \begin{cases} 1\ if\ (X_j - X_i) > 0 \\ 0\ if\ (X_j - X_i) = 0 \\ -1\ if\ (X_j - X_i) < 0 \end{cases} \quad (3)$$

213 where X_j and X_i are the values sorted by data sequence and n is the length of the time series.

214 The Z statistic is the standardized value of the trend, which is calculated with the following equations as
215 illustrated in Hannaford et al. (2013):

216 $$Z = \begin{cases} \frac{S-1}{\sqrt{Var(S)}}\ if\ S > 0 \\ 0\ if\ S = 0 \\ \frac{S+1}{\sqrt{Var(S)}}\ if\ S < 0 \end{cases} \quad (4)$$

The multi-temporal trend analysis approach was also adopted to analyse sensitivity of the period selected for calculation of the Pearson product moment correlations between Q_{MAX} time series and PCP_{MAX}, SME_{MAX} and SMN_{MAX} time series, respectively. Pearson *r* correlation coefficient measures the strength of a linear relationship between respective variables. Both multi-temporal trend and correlation analysis were carried out for the entire record length of each pair (Table 2).

2.6 Multi-temporal correlation analysis

We applied the Pearson correlations between the time series of flood magnitude (Q_{MAX}) and flood drivers (PCP_{MAX}, SMN_{MAX} and SME_{MAX}), as implemented by similar studies such as Lin et al. (2023), Venegas-Cordero et al. (2023) and Wu and Huang (2015). Additionally, we evaluated the sensitivity of the period, by detecting the correlation value for all possible combinations of starting and ending years with a minimum time window of 20 years.

2.7 Multiple linear regression

We determined the influence of climatic variables on Q_{MAX} time series, using a multiple linear regression in which maximum precipitation, soil moisture excess and snowmelt were used as the predictor variables of annual maximum flow, similar to the study implemented by Vicente-Serrano et al. (2019). A temporal multiple regression analysis was developed for each paired-catchment with the following equation:

$$Q \sim PCP + SME + SMN \quad (5)$$

where *Q*, *PCP*, *SME* and *SMN* are the annual maximum flow, precipitation, soil moisture excess and snowmelt, respectively.

We then calculated a time series of regression residuals using the observed and predicted Q_{MAX}, which was obtained from the regression model in equation 5. We applied the MK test with the Z-statistic and a p-value (at a 10% significance level) on the residual time series to evaluate possible changes in the role of

239 climatic variables or human factors (urbanization) on the annual maximum flow, following Vicente-
240 Serrano et al. (2019). We assume that the residual time series is not dependent on climate variables,
241 hence, statistically significant trends in residuals could be attributed to human factors (in our case
242 urbanization, for the urban catchments). In the paired-catchment context, the difference between Z values
243 of Q_{MAX} residual MK test between urban and non-urban catchments could also be attributed to the main
244 differing factor (imperviousness).

245 # 3. Results

246 ## 3.1 Imperviousness change

247 The analysis of the change in imperviousness indicator based on the GHS product for the period 1975-
248 2020 reveals a consistent upward pattern across all catchment pairs considered in the study (Fig. 3). The
249 change rate in this period was fairly constant for both urban and non-urban catchments. The disparities
250 between urban and non-urban catchments were steadily growing and particularly pronounced in the final
251 years of the analysed period, thus pointing to a potential influence in urbanization dynamics (Fig 3).

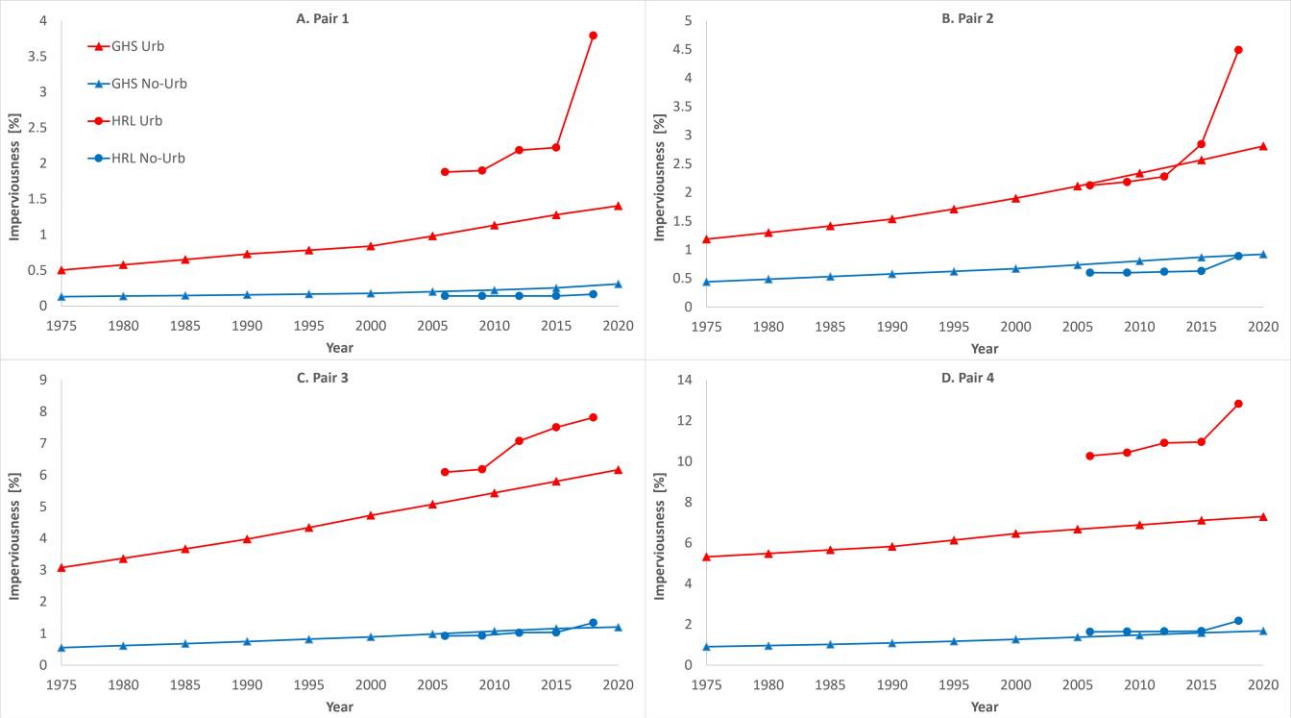

Fig 3: Changes in imperviousness (%) for all catchment pairs in the period 1975-2020. Red color refers to urban catchments and blue color to non-urban. Circles represent HRL data and triangles GHS.

The additional analysis based on the higher resolution of the HRL product for the shorter period 2006-2018 corroborates previous findings. However, the rate of change within 3-year intervals is not as stable as for the GHS product. Particularly, high increases reaching 1.7% were revealed for catchments U1 and U2 during the last interval 2015-2018.

3.2 Change point detection

The change point analysis for Q_{MAX} time series using the Pettitt test allowed us to detect one change point for both catchments U4 and N4 of the pair 4. The years 1983 and 1985 were the change point years for catchments U4 and N4, respectively (Fig. 4). In both cases an abrupt decrease in QMAX occurred in mid-1980s. Change points were detected for both urban and non-urban catchments and they occurred in neighbouring years. Therefore, we can draw the hypothesis that they could be caused by climatic rather than human factors. It should be noted that while pair 4 features the longest record length dating back to

1951, the other pairs have significantly shorter periods which perhaps made it harder to detect the change point in 1980s.

Consequently, in subsequent analysis for pair 4 we split the period into two sub-periods: 1951-1982 and 1984-2020 for U4, and 1951-1984 and 1986-2020 for N4.

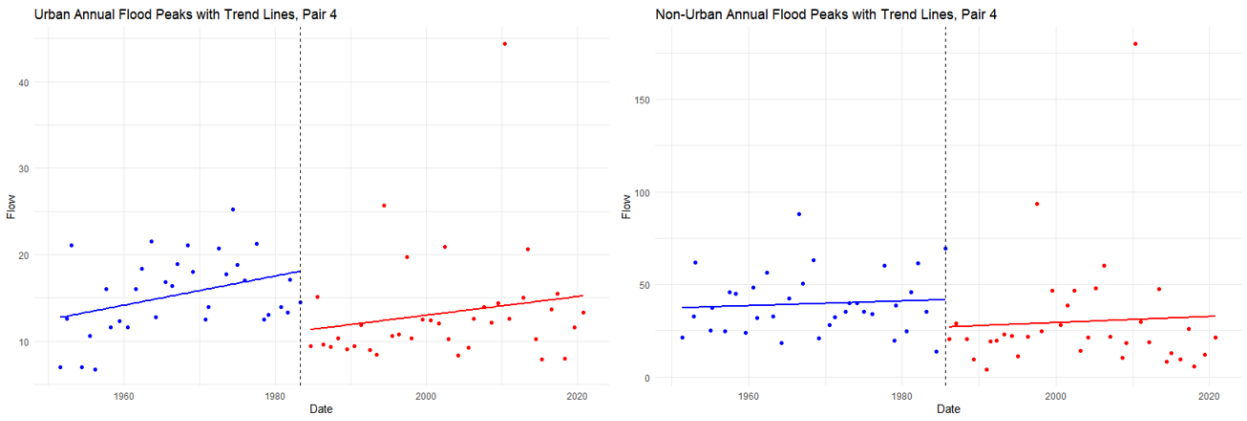

Fig 4: Change point detection using the Pettitt test for the catchment pair 4. Vertical dashed line represents change point years.

3.3 Detection of trends in QMAX

This section focuses on detection of monotonic trends for all catchments. The multi-temporal trend analysis results for Q_{MAX} for all paired catchments are shown in Fig. 5. The results confirm the sensitivity of MK test statistics to the period considered. There are clear differences between the urban and non-urban catchments. For catchment U1, a significant increasing trend was detected for most of combinations of starting and ending years. It was particularly strong for starting years in the period 1982-1992 and ending years in the period 2007-2018. However, no trends were detected for catchment N1 that belongs to the same pair, which suggests urbanization as a plausible factor to explain the increase in Q_{MAX} in U1 in such period.

The results for pair 2 showed similarities in flood trends between the urban (U2) and non-urban (N2) catchments. In both of them, trends were mostly non-significant, with a few exceptions that are similar in both catchments. Thus, in this case there is no evidence for the role of urbanization.

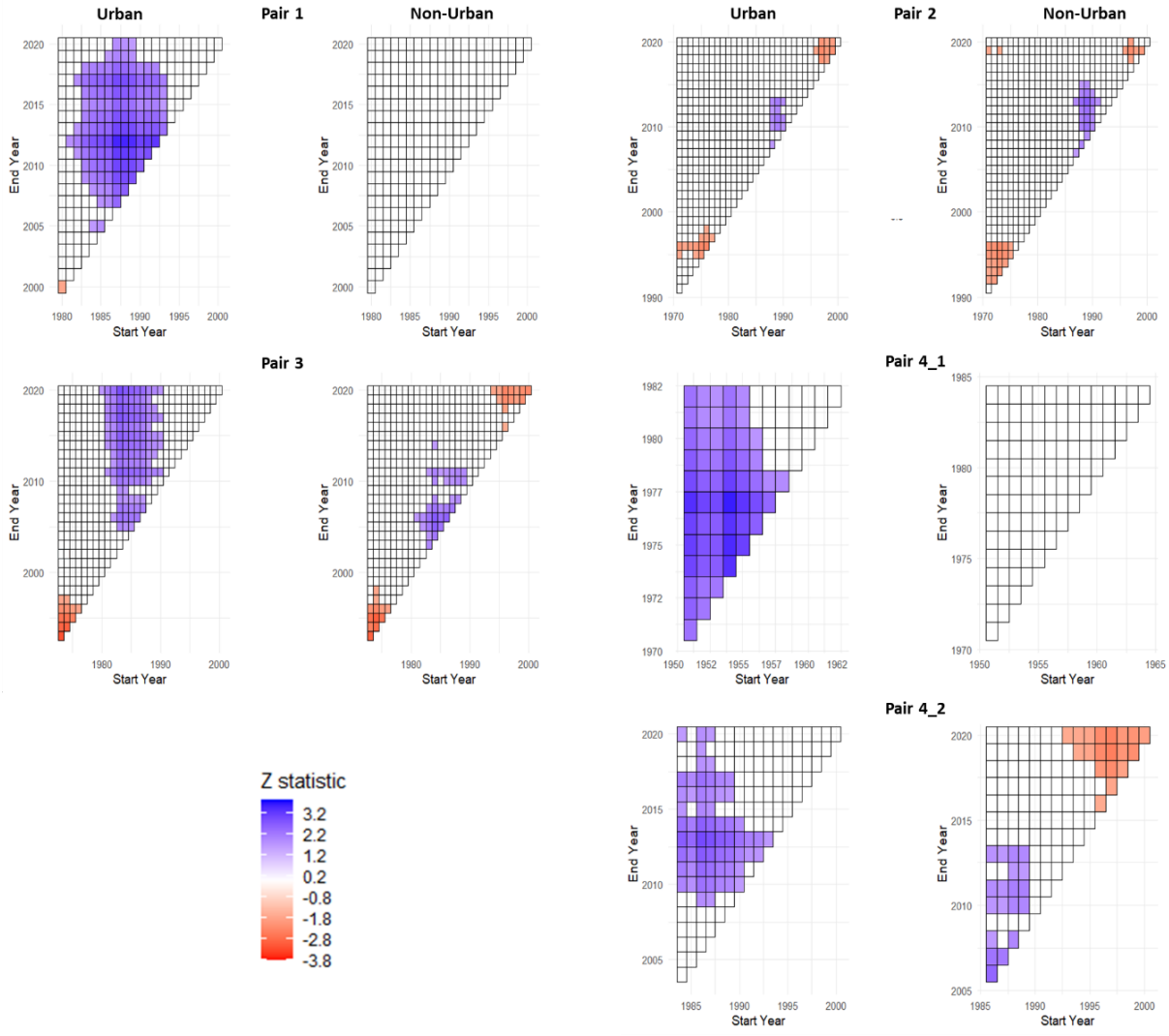

Fig. 5: Multi-temporal trend analysis for Q_{MAX} for all catchment pairs. The *x* and *y* axes represent the starting and ending years, respectively. Each pixel is colored according to the resulting Z statistic from the MK test and the p-value (pixels with p>10% are left blank). Red and blue colors represent decreasing and increasing trends, respectively.

For the catchment U3, Q_{MAX} trends are significantly positive across most sub-periods that start in the 1980s. However, trends were mostly non-significant for the same sub-periods for catchment N3 (apart from those ending before 2012). As in the case of the catchment pair 1, it suggests that urbanization could be a factor that could explain this differing behavior between the two catchments. Furthermore, the difference was more noticeable for sub-periods with ending years in the period 2015-2020, and thus most affected by urbanization process in catchment U3 (Fig. 3).

Finally, for the catchment pair 4, the catchment U4 exhibited a predominantly positive trend in Q_{MAX} for almost all possible combinations of starting and ending years during the sub-period 1 (1951-1982). No significant trends were detected for its paired non-urban catchment N4. Therefore, the difference between catchment behaviour could be attributed to urbanization. In the case of the sub-period 2 (1984-2020), the difference between U4 and N4 is not as evident, yet still noticeable. Increasing trends for the majority of sub-periods ending in years 2010-2020 were detected for the urban catchment U4 in the sub-period 2. In the case of its non-urban pair N4, the majority of trends were non-significant, although a few significant increasing trends were also detected for the sub-periods ending in years 2005-2013 and decreasing at the end of the years 2016-2020.

In summary, catchment pair 2 was the only with no evidence for the role of imperviousness on flood behavior changes.

3.4 Detection of trends in POT3

The multi-temporal trend analysis results for the magnitude of POT3 time series in all the paired catchments are shown in Fig. 6. To some extent, they corroborate previous findings with Q_{MAX}. The strongest evidence for the role of urbanization on floods estimated using the POT approach could be found for the catchment pair 4 in the sub-period 2. Some evidence can also be noticed for catchment pairs 1 and 3, although only for a limited number of combinations of starting and ending years. Quite surprisingly, the

non-urban catchment N2 shows an inverse behaviour in comparison with other non-urban catchments, exhibiting a positive trend for the periods starting in years 1980-1985. Thus, in this case the comparison with its paired catchment U2 leads to an opposite conclusion regarding the role of imperviousness compared to other pairs.

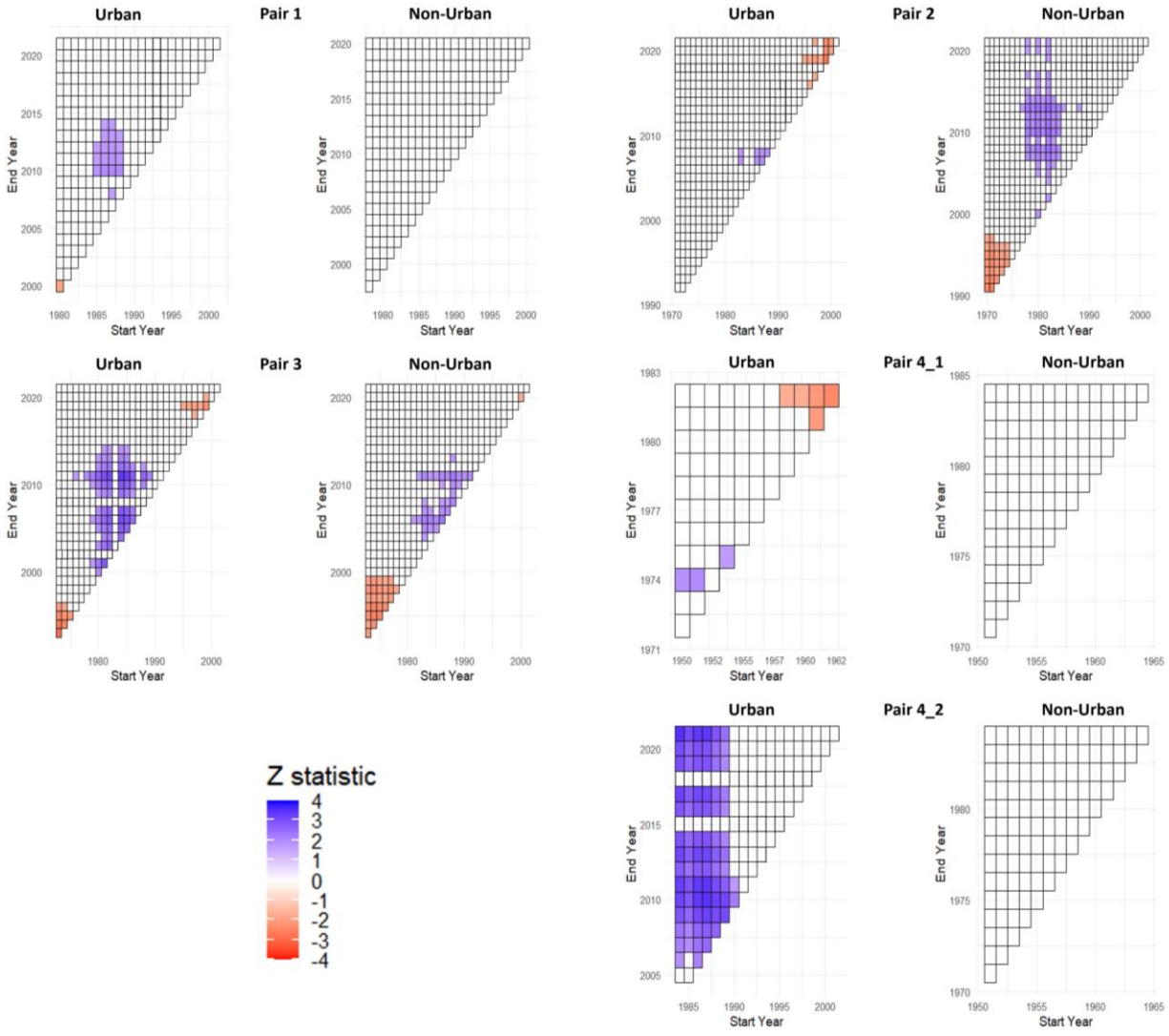

Fig. 6: Multi-temporal trend analysis for the POT3 magnitude time series for all catchment pairs. The *x* and *y* axes represent the starting and ending years, respectively. Each pixel is colored according to the resulting Z statistic from the MK test and the p value (pixels with p>10% are left blank). Red and blue colors represent decreasing and increasing trends, respectively.

3.4 Detection of trends in POT frequency

The frequency of flood events is determined based on the POT3F time series. Figure 7 illustrates the multi-temporal trend changes in the number of annual flood events that exceed a given threshold, as determined by the Poisson regression test. We observed that for the majority of time windows, no statistically significant changes in the flood frequency could be detected. The largest difference between the urban and non-urban catchments was found for the catchment pair 4, for which increases in flood frequency were detected for catchment U4, while no changes were found for catchment N4. For the remaining pairs the differences between urban and non-urban catchments was negligible.

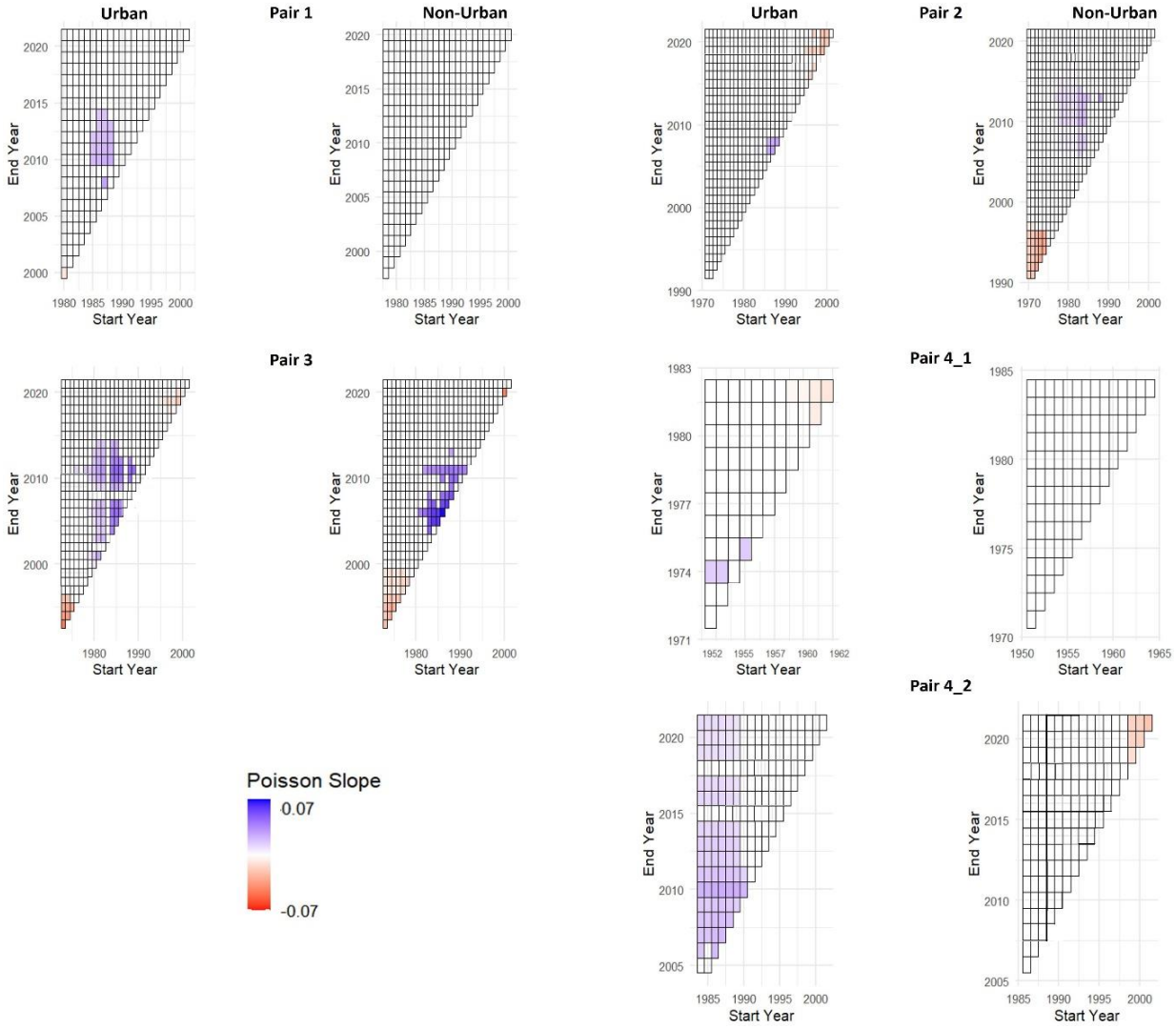

Fig. 7: Multi-temporal trend analysis for the POT3F time series for all catchment pairs. The x and y axes represent the starting and ending years, respectively. Each pixel is colored according to the resulting the Poisson regression test and the p value (pixels with p>10% are left blank). Red and blue colors represent decreasing and increasing trends, respectively.

3.5 Multi-temporal correlation

A comprehensive linear correlation analysis was conducted between Q_{MAX} and PCP_{MAX}, SME_{MAX}, and SMN_{MAX} for all possible combinations of starting and ending years within the time windows of data availability of each pair, to have a better insight into the role of climatic factors on flood generation. It could be expected that non-urban catchments will generally exhibit higher correlation coefficients than their paired urban catchments, as urbanization can be regarded as a confounding factor for the relationship between climate indices and floods. It was the case for catchment pair 1 (particularly strong for the soil moisture excess), pair 3 (precipitation) and pair 4 (precipitation and snow melt). In the case of pair 2, the patterns in correlation plots were largely similar for U2 and N2 catchments for SME and SNM, while for PCP the urban catchment exhibited significantly higher correlations. It is in line with previous findings showing no detected effect of urbanization for this pair.

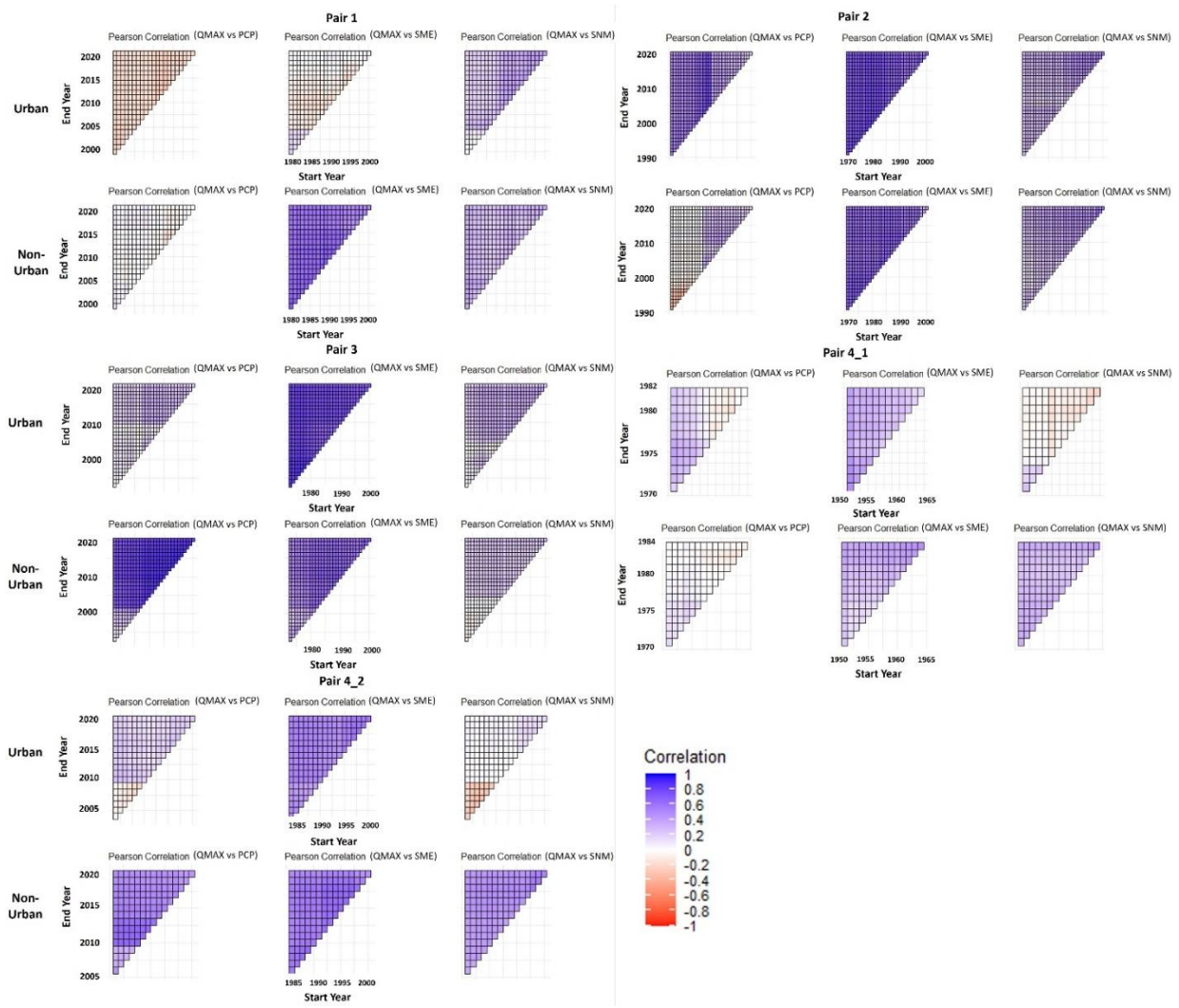

Fig. 8: Multi-temporal Pearson correlation analysis for Q_{MAX} against PCP_{MAX}, SME_{MAX} and SNM_{MAX} for all catchment pairs. The *y* axis shows the ending year and the x axis represents the starting year. Each pixel is colored according to the R value. Red and blue colors represent negative and positive correlations, respectively.

3.6 Multiple regression with climate variables

The results of the multiple regression analysis between Q_{MAX} and climate indices for each pair are presented in Table 4. The R^2 of the multiple regression model varied considerably between catchments, ranging between 0.07 (U1) and 0.62 (U3 and N3). The comparison of coefficients of determination for pairs 1 and 4_2 (sub-period 2) shows that non-urban catchments exhibits stronger relationships between floods

and climate indices than the urban ones. A more detailed dissection of the R^2 values from multiple regression to its individual components reveals certain patterns. For example, precipitation is not the dominant explaining factor in any of the studied catchments. Soil moisture excess and snow melt appear to have higher exploratory power.

Table 4: Results of the multiple regression analysis between Q_{MAX} and PCP, SME and SMN climate variables.

Pair ID	Catchment	R^2 (multiple)	R^2 (PCP)	R2 (SME)	R^2 (SMN)	p value (residuals)	z (residuals)
1	U1	0.07	0.02	-0.01	-0.02	0.15	1.44
	N1	0.41	0.01	0.38	0.25	0.71	0.37
2	U2	0.57	0.04	0.31	0.44	0.76	0.30
	N2	0.50	0.14	0.49	0.40	0.40	-0.84
3	U3	0.62	-0.01	0.58	0.58	0.45	-0.75
	N3	0.62	0.35	0.09	0.56	0.09	-1.66
4	U4_1	0.22	-0.01	0.11	0.17	0.11	1.57
	N4_1	0.22	0.01	0.17	0.05	0.83	-0.21
	U4_2	0.31	-0.02	0.24	0.28	0.94	0.06
	N4_2	0.50	0.22	0.23	0.28	0.90	0.11

In addition, the analysis of residuals did not show any significant trends (with an exception of catchment N3 having a statistically significant decreasing trend at p = 0.1; see Fig. S2-S6 in Electronic Supplementary Material). Lack of statistically significant increasing trends for urban catchments could be interpreted as the lack of an effect of imperviousness in flood changes. However, taking the context of the paired-catchment approach, it makes sense to compare z values of residuals for each pair. The differences in residuals are for all cases quite high and positive except for pair 4 in sub-period 2, thus providing an indirect evidence supporting the hypothesis about the effect of urbanization on floods.

4. Discussion

We conducted a comprehensive array of statistical methods to investigate the impact of urbanization on fluvial floods in Poland. While discerning flood trends is a relatively simple task, attributing these trends to urbanization presents a challenge due to the intricate interplay of various factors. In this context, the

paired catchments approach provides a valuable advantage by comparing basins with different levels of imperviousness, allowing for the quantification of the impact of urbanization. This method effectively isolates the effects of urbanization within a specific region by assessing observed streamflow, precipitation, soil moisture excess, and snowmelt statistics in paired catchments.

It is important to note that the nature of evidence pertaining to the effect of urbanization on floods in our study is, at best, moderate. One potential explanation for this observation is that the rate of imperviousness increase in the studied urban catchments may not have been as high as observed worldwide. For example, Requena et al. (2017) who studied the potential effect of urbanization on the peak flows in a paired catchment study in the northwest of England, the imperviousness in an urban catchment increased by 7% during 30 years which is much higher than in any of our urban catchments. Prosdocimi et al. (2015) also detected a higher increase (10.1%) over 40 years in an urban catchment in the UK. In Finland, a catchment has rapidly developed from a rural area to urban in 2001–2006, especially for a residential development (Guan et al., 2015). Finally, in the USA, in a historical study, a non-significant increase of annual maximum flows has been detected for a catchment with a higher increase (20%) of imperviousness in around two decades (Brun and Band, 2000). In our study, a significant increase in Q_{MAX} was observed for most pairs, with the exception of catchment pair 2. This finding aligns with broader flood trends reported by Venegas et al. (2022) and Venegas et al. (2023). While climate variables are acknowledged as primary contributors to streamflow variability, our analysis, utilizing paired catchments, distinguishes the specific impacts of urbanization and changing climate on floods. This is achieved by comparing areas influenced by urban factors with non-urban catchments. Requena et al. (2017) found positive trend in an urban area, similar as our results. Also, they mentioned that the changes in the annual series would be mainly due to changes in summer, where the extreme precipitation events are the main element associated with the summer time (Requena et al., 2017). In our study the soil moisture excess and snowmelt have a stronger effect among the climatic drivers. This aspect can be associated with a

recent study that identified the snowmelt as the principal flood mechanism in Poland, but analysis in recent decades shows tracks of decreasing snowmelt and increasing on soil moisture excess (Venegas-Cordero et al., 2023). In addition, peak flows in urban catchments tend to be higher, so the time to peak is shorter than in rural catchments (Akter et al., 2018).

The relationship between rainfall and flooding is more complex on a larger scale in non-urban areas, as indicated by Ivancic et al. (2015). This complexity is reflected in the multi-temporal correlation between Q_{MAX} and extreme precipitation, where the highest values are observed in urban areas. For example, Gu et al., (2019) and Yang et al., (2017), who studied the urbanization impact on extreme rainfall events (annual an seasonal) in China, found that urbanization noticeably affects the regional patterns of rainfall, impacting intensity, amount and spatial distribution. Additionally, soil moisture excess seems to be the principal factor in the multiple regression analysis, where the highest values of R^2 were found for the urban catchment over all pairs, which agreed with the previous study of Wasko and Nathan (2019). They studied the effect of precipitation and soil moisture on patterns in flooding and mentioned that modifications in soil moisture emerge as the prevailing element influencing the identified shifts in flooding dynamics.

One of the limitations of our study was that the sample size of catchments used in the analysis was relatively low. This limitation is a direct result of the selected methodological approach, which required the identification of paired catchments that met specific criteria such as appropriate size, divergent urbanization characteristics within each pair, sufficient length of flow record and a good overlay of flow data availability between urban and non-urban catchments. In the context of Polish conditions, our identification process produced only four suitable pairs. In particular, the identified urban catchments did not intersect with any of the major metropolitan areas in Poland, such as Warsaw, Kraków, Wrocław, Łódź or Poznań. It is interesting to note that the increase in imperviousness in these urban centers might have been more pronounced than in our selected catchments. However, catchments located in these urban

areas lack flow gauges or existing gauges do not have sufficient records, which made it impossible to include them in our study.

5. Conclusions

This study examined changes in imperviousness, flood trends, and climate interactions in four catchment pairs in Poland between 1975 and 2020. The results reveal a consistent upward trajectory in imperviousness in all pairs (much stronger in urban catchments compared to their non-urban counterparts), indicating a significant trend in urbanization dynamics. Change point detection, using the Pettitt test, helped to identify changes in Q_{MAX} time series in both urban and non-urban watersheds for only one catchment pair.

Analysis of Q_{MAX} trends revealed notable variations between urban and non-urban catchments. The pair 2 distinguished itself by showing no discernible evidence of imperviousness influencing changes in flood behavior. Application of the POT approach further corroborated the impact of imperviousness on flooding, particularly evident for catchment pair 4 during the later period (1986-2020), with additional evidence observed for catchment pairs 1 and 3.

Flood frequency analysis (POT3F) showed a significant difference between urban and non-urban catchments for only one catchment pair (number 4). Multitemporal correlation analysis revealed variable relationships between flood magnitude and climatic variables, with non-urban catchments showing higher correlations. Finally, multiple regression analysis underscored the intricate relationships between flooding and climate indices, with non-urban catchments consistently showing higher coefficients of determination than their urban counterparts. The residual analysis, although lacking statistically significant increasing trends for most urban catchments, indicated differences that indirectly supported the hypothesis of the effect of urbanization on flooding. Understanding flood dynamics is crucial for formulating effective flood risk management strategies in both urban and non-urban environments.

Author contributions

NVC: Conceptualization, Investigation, Methodology, Software, Validation, Formal analysis, Visualization, Writing – original draft, Writing – review & editing. **LM**: Conceptualization, Writing – original draft, Writing – review & editing. **MP**: Conceptualization, Investigation, Writing – original draft, Writing – review & editing, Supervision.

Declaration of Competing Interest

No conflicts of interest were reported by the authors.

Acknowledgements

This study is supported financially by the National Science Centre (NCN) in Poland under the research project "ATtribution of changes in RIver FLOods in Poland (ATRIFLOP)", grant 2022/45/N/ST10/03551. The authors acknowledge funding from the project PID2019-107027RB-I00 'SAFERDAMS: Assessment of the impact of climate change on hydrological dam safety' of the Spanish Ministry of Science and Innovation (PID2019-107027RB-I00 / AEI / 10.13039/501100011033). This version of the article had been submitted to Stochastic Environmental Research and Risk Assessment and, after peer review process, was accepted for publication in this journal on 30 March 2024. The Version of Record is available online at: https://doi.org/10.1007/s00477-024-02717-z

References

Akter, T., Quevauviller, P., Eisenreich, S. J. and Vaes, G. (2018). Impacts of climate and land use changes on flood risk management for the Schijn River, Belgium. Environmental science & policy, 89, 163-175.

Allan, R. P., Barlow, M., Byrne, M. P., Cherchi, A., Douville, H., Fowler, H. J. and Zolina, O. (2020). Advances in understanding large-scale responses of the water cycle to climate change. Annals of the New York Academy of Sciences, 1472(1), 49-75.

Aryal, Y.N., Villarini, G., Zhang, W. and Vecchi, G.A. (2018). Long term changes in flooding and heavy rainfall associated with North Atlantic tropical cyclones: Roles of the North Atlantic Oscillation and El Niño-Southern Oscillation. Journal of Hydrology, 559: 698-710.

Bayazıt, Y., Koç, C. and Bakış, R. (2021). Urbanization impacts on flash urban floods in Bodrum Province, Turkey. Hydrological Sciences Journal, 66(1): 118-133.

Beckers, A., Dewals, B., Erpicum, S., Dujardin, S., Detrembleur, S., Teller, J. and Archambeau, P. (2013). Contribution of land use changes to future flood damage along the river Meuse in the Walloon region. Natural Hazards and Earth System Sciences, 13(9), 2301-2318.

Berghuijs, W.R., Harrigan, S., Molnar, P., Slater, L.J. and Kirchner, J.W. (2019). The Relative Importance of Different Flood-Generating Mechanisms Across Europe. Water Resources Research, 55(6): 4582-4593.

Bian, G., Du, J., Song, M., Zhang, X., Zhang, X., Li, R. and Xu, C. Y. (2020). Detection and attribution of flood responses to precipitation change and urbanization: a case study in Qinhuai River Basin, Southeast China. Hydrology Research, 51(2), 351-365.

Bosch, J.M. and Hewlett, J. (1982). A review of catchment experiments to determine the effect of vegetation changes on water yield and evapotranspiration. Journal of hydrology, 55(1-4): 3-23.

Brody, S., Blessing, R., Sebastian, A. and Bedient, P. (2014). Examining the impact of land use/land cover characteristics on flood losses. Journal of Environmental Planning and Management, 57(8): 1252-1265.

Brun, S. E. and Band, L. E. (2000). Simulating runoff behavior in an urbanizing watershed. Computers, environment and urban systems, 24(1), 5-22.

Brunner, M. I., Swain, D. L., Wood, R. R., Willkofer, F., Done, J. M., Gilleland, E. and Ludwig, R. (2021). An extremeness threshold determines the regional response of floods to changes in rainfall extremes. Communications Earth & Environment, 2(1), 173..

Bulti, D.T. and Abebe, B.G. (2020). A review of flood modeling methods for urban pluvial flood application. Modeling earth systems and environment, 6: 1293-1302.

Davenport, F.V., Herrera-Estrada, J.E., Burke, M. and Diffenbaugh, N.S. (2020). Flood size increases nonlinearly across the western United States in response to lower snow-precipitation ratios. Water Resources Research, 56(1): e2019WR025571.

Depietri, Y., Renaud, F.G. and Kallis, G. (2012). Heat waves and floods in urban areas: a policy-oriented review of ecosystem services. Sustainability Science, 7(1): 95-107.

Du, S., Van Rompaey, A., Shi, P. and Wang, J.a. (2015). A dual effect of urban expansion on flood risk in the Pearl River Delta (China) revealed by land-use scenarios and direct runoff simulation. Natural Hazards, 77: 111-128.

Fletcher, T. D., Andrieu, H. and Hamel, P. (2013). Understanding, management and modelling of urban hydrology and its consequences for receiving waters: A state of the art. Advances in water resources, 51, 261-279.

Francipane, A., Pumo, D., Sinagra, M., La Loggia, G. and Noto, L.V. (2021). A paradigm of extreme rainfall pluvial floods in complex urban areas: the flood event of 15 July 2020 in Palermo (Italy). Nat. Hazards Earth Syst. Sci., 21(8): 2563-2580.

Gao, Y., Chen, J., Luo, H. and Wang, H. (2020). Prediction of hydrological responses to land use change. Science of the Total Environment, 708, 134998.

Giorgi, F., Raffaele, F. and Coppola, E. (2019). The response of precipitation characteristics to global warming from climate projections. Earth System Dynamics, 10(1): 73-89.

Gu, X., Zhang, Q., Li, J., Singh, V. P. and Sun, P. (2019). Impact of urbanization on nonstationarity of annual and seasonal precipitation extremes in China. Journal of Hydrology, 575, 638-655.

Guan, M., Sillanpää, N. and Koivusalo, H. (2015). Modelling and assessment of hydrological changes in a developing urban catchment. Hydrological Processes, 29(13), 2880-2894.

Guerreiro, S.B., Dawson, R.J., Kilsby, C., Lewis, E. and Ford, A., 2018. Future heat-waves, droughts and floods in 571 European cities. Environmental Research Letters, 13(3): 034009.

Hannaford, J., Buys, G., Stahl, K. and Tallaksen, L. (2013). The influence of decadal-scale variability on trends in long European streamflow records. Hydrology and Earth System Sciences, 17(7): 2717-2733.

Hannaford, J., Mastrantonas, N., Vesuviano, G. and Turner, S. (2021). An updated national-scale assessment of trends in UK peak river flow data: how robust are observed increases in flooding? Hydrology Research, 52(3): 699-718.

Hebbert, M. (2012). Cities and Climate Change (Global Report on Human Settlements 2011). JSTOR.

Hodgkins, G. A., Whitfield, P. H., Burn, D. H., Hannaford, J., Renard, B., Stahl, K. and Wilson, D. (2017). Climate-driven variability in the occurrence of major floods across North America and Europe. Journal of Hydrology, 552, 704-717.

Hoeppe, P. (2016). Trends in weather related disasters – Consequences for insurers and society. Weather and Climate Extremes, 11: 70-79.

Ivancic, T. J. and Shaw, S. B. (2015). Examining why trends in very heavy precipitation should not be mistaken for trends in very high river discharge. Climatic Change, 133, 681-693.

Jiang, S., Zheng, Y., Wang, C. and Babovic, V. (2022). Uncovering Flooding Mechanisms Across the Contiguous United States Through Interpretive Deep Learning on Representative Catchments. Water Resources Research, 58(1): e2021WR030185.

Jodar-Abellan, A., Valdes-Abellan, J., Pla, C. and Gomariz-Castillo, F. (2019). Impact of land use changes on flash flood prediction using a sub-daily SWAT model in five Mediterranean ungauged watersheds (SE Spain). Science of the Total Environment, 657, 1578-1591.

Kendall, M. (1975). Rank correlation methods, book series, Charles Griffin. Oxford University Press, USA, London.

Kishtawal, C. M., Niyogi, D., Tewari, M., Pielke Sr, R. A. and Shepherd, J. M. (2010). Urbanization signature in the observed heavy rainfall climatology over India. International journal of climatology, 30(13), 1908-1916.

Kreibich, H., Di Baldassarre, G., Vorogushyn, S., Aerts, J. C., Apel, H., Aronica, G. T. and Merz, B. (2017). Adaptation to flood risk: Results of international paired flood event studies. Earth's Future, 5(10), 953-965..

Kundzewicz, Z. W., Kanae, S., Seneviratne, S. I., Handmer, J., Nicholls, N., Peduzzi, P. and Sherstyukov, B. (2014). Flood risk and climate change: global and regional perspectives. Hydrological Sciences Journal, 59(1), 1-28.

Kundzewicz, Z.W. and Robson, A.J. (2004). Change detection in hydrological records—a review of the methodology/revue méthodologique de la détection de changements dans les chroniques hydrologiques. Hydrological sciences journal, 49(1): 7-19.

Lang, M., Ouarda, T.B. and Bobée, B. (1999). Towards operational guidelines for over-threshold modeling. Journal of hydrology, 225(3-4): 103-117.

Lin, J., Zhang, W., Wen, Y. and Qiu, S. (2023). Evaluating the association between morphological characteristics of urban land and pluvial floods using machine learning methods. Sustainable Cities and Society, 99, 104891.

Madsen, H., Lawrence, D., Lang, M., Martinkova, M. and Kjeldsen, T. (2014). Review of trend analysis and climate change projections of extreme precipitation and floods in Europe. Journal of Hydrology, 519: 3634-3650.

Madsen, H., Rasmussen, P.F. and Rosbjerg, D. (1997). Comparison of annual maximum series and partial duration series methods for modeling extreme hydrologic events: 1. At-site modeling. Water resources research, 33(4): 747-757.

Mallakpour, I. and Villarini, G. (2015). The changing nature of flooding across the central United States. Nature Climate Change, 5(3): 250-254.

Mangini, W., Viglione, A., Hall, J., Hundecha, Y., Ceola, S., Montanari, A. and Parajka, J. (2018). Detection of trends in magnitude and frequency of flood peaks across Europe. Hydrological Sciences Journal, 63(4), 493-512.

Mann, H.B. (1945). Nonparametric tests against trend. Econometrica: Journal of the econometric society: 245-259.

Marcinkowski, P., Kardel, I., Płaczkowska, E., Giełczewski, M., Osuch, P., Okruszko, T., Venegas-Cordero., Ignar, S. and Piniewski, M. (2021). High-resolution simulated water balance and streamflow data set for 1951–2020 for the territory of Poland. Geoscience Data Journal, 10(2), 195-207.

McGrane, S. J. (2016). Impacts of urbanisation on hydrological and water quality dynamics, and urban water management: a review. Hydrological Sciences Journal, 61(13), 2295-2311.

Mediero, L., Santillán, D., Garrote, L. and Granados, A. (2014). Detection and attribution of trends in magnitude, frequency and timing of floods in Spain. Journal of Hydrology, 517: 1072-1088.

Mediero, L., Soriano, E., Oria, P., Bagli, S., Castellarin, A., Garrote, L. and Schröter, K. (2022). Pluvial flooding: High-resolution stochastic hazard mapping in urban areas by using fast-processing DEM-based algorithms. Journal of Hydrology, 608, 127649.

Mou, Y., Gao, X., Yang, Z., Xu, T. and Feng, J. (2022). Variation characteristics and the impact of urbanization of extreme precipitation in Shanghai. Scientific Reports, 12(1): 17618.

Pesaresi, M. and Politis, P. (2022). GHS-BUILT-S R2022A-GHS Built-Up Surface Grid, Derived from Sentinel-2 Composite and Landsat, Multitemporal (1975–2030). European Commission, Joint Research Centre (JRC) Sevilla, Spain.

Pettitt, A.N. (1979). A non-parametric approach to the change-point problem. Journal of the Royal Statistical Society: Series C (Applied Statistics), 28(2): 126-135.

Piniewski, M., Marcinkowski, P. and Kundzewicz, Z.W. (2018). Trend detection in river flow indices in Poland. Acta Geophysica, 66(3): 347-360.

Piniewski, M., Szcześniak, M., Kardel, I., Chattopadhyay, S. and Berezowski, T. (2021). G2DC-PL+: a gridded 2 km daily climate dataset for the union of the Polish territory and the Vistula and Odra basins. Earth System Science Data, 13(3): 1273-1288.

Pińskwar, I., Choryński, A. and Graczyk, D. (2023). Risk of Flash Floods in Urban and Rural Municipalities Triggered by Intense Precipitation in Wielkopolska of Poland. International Journal of Disaster Risk Science, 1-18.

Prein, A. F., Rasmussen, R. M., Ikeda, K., Liu, C., Clark, M. P. and Holland, G. J. (2017). The future intensification of hourly precipitation extremes. Nature climate change, 7(1), 48-52.

Prosdocimi, I., Kjeldsen, T.R. and Miller, J.D. (2015). Detection and attribution of urbanization effect on flood extremes using nonstationary flood-frequency models. Water Resources Research, 51(6): 4244-4262.

Requena, A. I., Prosdocimi, I., Kjeldsen, T. R. and Mediero, L. (2017). A bivariate trend analysis to investigate the effect of increasing urbanisation on flood characteristics. Hydrology Research, 48(3), 802-821.

Ruiz-Villanueva, V., Stoffel, M., Wyżga, B., Kundzewicz, Z. W., Czajka, B. and Niedźwiedź, T. (2016). Decadal variability of floods in the northern foreland of the Tatra Mountains. Regional Environmental Change, 16, 603-615.

Salavati, B., Oudin, L., Furusho-Percot, C. and Ribstein, P. (2016). Modeling approaches to detect land-use changes: Urbanization analyzed on a set of 43 US catchments. Journal of Hydrology, 538, 138-151.

Sen, P.K. (1968). Estimates of the regression coefficient based on Kendall's tau. Journal of the American statistical association, 63(324): 1379-1389.

Serinaldi, F., Kilsby, C.G. and Lombardo, F. (2018). Untenable nonstationarity: An assessment of the fitness for purpose of trend tests in hydrology. Advances in Water Resources, 111: 132-155.

Shao, M., Zhao, G., Kao, S. C., Cuo, L., Rankin, C. and Gao, H. (2020). Quantifying the effects of urbanization on floods in a changing environment to promote water security—A case study of two adjacent basins in Texas. Journal of Hydrology, 589, 125154.

Skougaard Kaspersen, P., Høegh Ravn, N., Arnbjerg-Nielsen, K., Madsen, H. and Drews, M. (2017). Comparison of the impacts of urban development and climate change on exposing European cities to pluvial flooding. Hydrology and Earth System Sciences, 21(8): 4131-4147.

Smith, A., Tetzlaff, D., Marx, C. and Soulsby, C. (2023). Enhancing urban runoff modelling using water stable isotopes and ages in complex catchments. Hydrological Processes, 37(2): e14814.

Szeląg, B., Suligowski, R., Drewnowski, J., De Paola, F., Fernandez-Morales, F. J. and Bąk, Ł. (2021). Simulation of the number of storm overflows considering changes in precipitation dynamics and the urbanisation of the catchment area: A probabilistic approach. Journal of Hydrology, 598, 126275.

Szwagrzyk, M., Kaim, D., Price, B., Wypych, A., Grabska, E. and Kozak, J. (2018). Impact of forecasted land use changes on flood risk in the Polish Carpathians. Natural Hazards, 94, 227-240.

Tabari, H. (2020). Climate change impact on flood and extreme precipitation increases with water availability. Scientific reports, 10(1): 1-10.

Tramblay, Y., Mimeau, L., Neppel, L., Vinet, F. and Sauquet, E. (2019). Detection and attribution of flood trends in Mediterranean basins. Hydrology and Earth System Sciences, 23(11): 4419-4431.

Van Loon, A. F., Rangecroft, S., Coxon, G., Breña Naranjo, J. A., Van Ogtrop, F. and Van Lanen, H. A. (2019). Using paired catchments to quantify the human influence on hydrological droughts. Hydrology and Earth System Sciences, 23(3), 1725-1739.

Venegas-Cordero, N., Cherrat, C., Kundzewicz, Z.W., Singh, J. and Piniewski, M. (2023). Model-based assessment of flood generation mechanisms over Poland: The roles of precipitation, snowmelt, and soil moisture excess. Science of The Total Environment: 164626.

Venegas-Cordero, N., Kundzewicz, Z.W., Jamro, S. and Piniewski, M. (2022). Detection of trends in observed river floods in Poland. Journal of Hydrology: Regional Studies, 41: 101098.

Vicente-Serrano, S. M., Peña-Gallardo, M., Hannaford, J., Murphy, C., Lorenzo-Lacruz, J., Dominguez-Castro, F., and Vidal, J. P. (2019). Climate, irrigation, and land cover change explain streamflow trends in countries bordering the northeast Atlantic. Geophysical Research Letters, 46(19), 10821-10833.

Villarini, G., Serinaldi, F., Smith, J.A. and Krajewski, W.F. (2009). On the stationarity of annual flood peaks in the continental United States during the 20th century. Water Resources Research, 45(8).

Villarini, G., Smith, J.A., Ntelekos, A.A. and Schwarz, U. (2011). Annual maximum and peaks-over-threshold analyses of daily rainfall accumulations for Austria. Journal of Geophysical Research: Atmospheres, 116(D5).

Vormoor, K., Lawrence, D., Schlichting, L., Wilson, D. and Wong, W.K. (2016). Evidence for changes in the magnitude and frequency of observed rainfall vs. snowmelt driven floods in Norway. Journal of Hydrology, 538: 33-48.

Wang, X., Kinsland, G., Poudel, D. and Fenech, A. (2019). Urban flood prediction under heavy precipitation. Journal of Hydrology, 577: 123984.

Wasko, C. and Nathan, R. (2019). Influence of changes in rainfall and soil moisture on trends in flooding. Journal of Hydrology, 575: 432-441.

Wu, C., and Huang, G. (2015). Changes in heavy precipitation and floods in the upstream of the Beijiang River basin, South China. International Journal of Climatology, 35(10), 2978-2992.

Yang, X. J., Xu, Z. X., Liu, W. F. and Liu, L. (2017). Spatiotemporal characteristics of extreme precipitation at multiple timescales over Northeast China during 1961–2014. Journal of Water and Climate Change, 8(3), 535-556.

Zhang, H., Wang, B., Li Liu, D., Zhang, M., Leslie, L. M. and Yu, Q. (2020). Using an improved SWAT model to simulate hydrological responses to land use change: A case study of a catchment in tropical Australia. Journal of Hydrology, 585, 124822.